Int. J. Nanosci. Nanotechnol., Vol. 9, No. 2, June 2013, pp. 85-94

# Effect of Nano-$TiO_2$ Particles on the Corrosion Behavior of Chromium-Based Coatings

**M. Noroozifar*, M. Khorasani-Motlagh, Z. Yavari**

Department of Chemistry, University of Sistan & Baluchestan, Zahedan, I. R. Iran

(*) Corresponding author: mnoroozifar@chem.usb.ac.ir
*(Received:28 Jan. 2013 and Accepted: 01 May 2013)*

***Abstract:***
*Nanosized $TiO_2$ particles were prepared by sol–gel method. The $TiO_2$ particles were co-deposited with chromium using electrodeposition technique. In investigating of coating surfaces by scanning electron microscope (SEM), the results showed that the morphology of the coating surface was changed by adding $TiO_2$ nanoparticles to the chromium coating. The corrosion behavior of the coatings was assessed by polarization technique in four media such as seawater, pipeline water, distilled water and 3.5% NaCl solution. The results showed that adding the $TiO_2$ nanoparticles into chromium coating, caused a decrease in current and rate of corrosion, and so increased the period of conservation from cupric undercoat.*
***Keywords:*** *$TiO_2$ Nanoparticles, Corrosion, Composite Coating, Chromium Electroplating, Tafel Curve.*

## 1. INTRODUCTION

Copper and copper-based alloys are widely used in a great variety of applications, such as industrial equipment, building construction, electricity, electronics, coinage, ornamental parts, water treatment, etc [1].
Copper is widely used for tubing and piping in the distribution systems of drinking water throughout the world. Laws and standards have been issued in many countries to control copper levels in drinking water [2]. Corrosion of copper and its inhibition in a wide variety of media, particularly when they contain chloride ions, have attracted attention of a number of investigators [3]. Copper corrosion is the result of the loss of solid copper metal to solution. This occurs when electrons are lost by the base metal, and the solid phase is transformed into soluble, dissolved cuprous ($Cu^+$) and/or cupric ($Cu^{2+}$) ions. During metal corrosion in drinking water, chemical oxidation occurs at anodes where electrons are released. Alternately, chemical reduction (the gain of the electrons) occurs at the cathode [4].
Black chromium coatings are noteworthy as an alternative to either light chromium or black nickel deposits owing to their enhanced corrosion resistance. Traditional Cr-matrix coatings electrodeposited from Cr(VI) baths have been widely used for decoration and anti-corrosion. Electrodeposition of Cr(VI) needs to be replaced by another material system due to the intense toxicity and carcinogenicity of Cr(VI). Trivalent Cr plating is considered to be a promising replacement technology for hexavalent Cr plating [5]. Hexavalent chromium plating has been commercialized many years before. The main advantage of Cr(III) plating bath in comparison with a Cr(VI)-bath is that $Cr^{3+}$ ions are nontoxic environmentally benign[6].
Much attention has been focused on the development of ceramic/metal nanocomposites because such

materials offer outstanding mechanical and multifunctional properties. Composite coatings are produced by co-deposition of inert particles into a metal matrix from an electrolytic or electroless bath being considered as metal matrix composite (MMC) coating [7]. Particle-reinforced metal matrix composites generally exhibit wide engineering applications due to their high hardness, good wear resistance, and corrosion resistance compared to pure metal or alloy [8].

Composite electroplating has been identified to be a technologically feasible and economically superior technique for the preparation of such kind of composites, owing to the advantages including precisely controlled near ambient temperature operation, conducted at a normal pressure, low cost, rapid deposition rate, capability to handle complex geometries, and simple scale-up with easily maintained equipment [9].

In the last three decades, micro and nano-sized inorganic inert particles with metal or alloy such as SiC [10], $ZrO_2$ [11], $Al_2O_3$ [8], $TiO_2$ [9], $CeO_2$[12], nano-diamond [13] have been reported by electroplating technique.

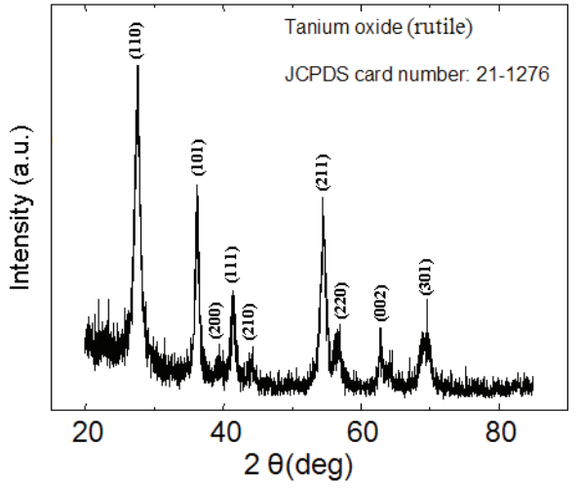


***Figure 1**: XRD powder patterns of prepared nanocrystalline $TiO_2$ rutile.*

In this work, $TiO_2$ nanoparticles were added to the chromium metallic coatings and their effects on substrate protection were studied. Cr-$TiO_2$ nanocomposite coating was obtained by electrochemical deposition of $TiO_2$ nanoparticles in the chromium plating bath including a copper piece as cathode. The corrosion behaviors of the mentioned composite coating and the chromium one on the copper surface were compared with the bare copper surface by electrochemical polarization. The results showed that the simultaneous Cr and nano $TiO_2$ deposition was led to the preparation of a uniform coating with better corrosion properties.

## 2. EXPERIMENTAL

### 2.1. Materials

Titanium(IV) chloride (99.9%) and benzyl alcohol (99.8%, anhydrous) were obtained from Merck. All reagents were prepared from analytical reagent grade chemicals unless specified otherwise and purchased from Merck Company. All aqueous solutions were prepared with double-distilled water (DDW). A suitable volume of acid (nitric acid) or base (sodium hydroxide) solution was added to adjust pH that was measured with pH-meter.

### 2.2. Instrumentation

The morphology of the sorbent was observed by means of a Philips XL30 scanning electron microscopy (SEM) with a maximum voltage 30 kV. A Metrohm 632 pH-meter with a Metrohm double junction glass electrode was used for pH adjustment. X-ray powder diffraction (XRD) analysis was conducted at 298 K on a Philips analytical PC-APD X-ray diffractometre with graphite monochromatic Cu Kα radiation (λ = 1.54056 Å) to verify the formation of products. JCPDS-ICDD standard files software were used to determine the phases.

The electrochemical polarization for the prepared coatings were carried out in four media such as seawater, Zahedan pipeline water, distilled water and 3.5% NaCl solution without pH control or aeration by using a SAMA500 (Sama research center, Esfahan, Iran). A three-electrode cell including a saturated calomel reference electrode (SCE), a platinum auxiliary electrode, and the sample as working electrode was used in the experiments. The working electrode (samples) were enveloped

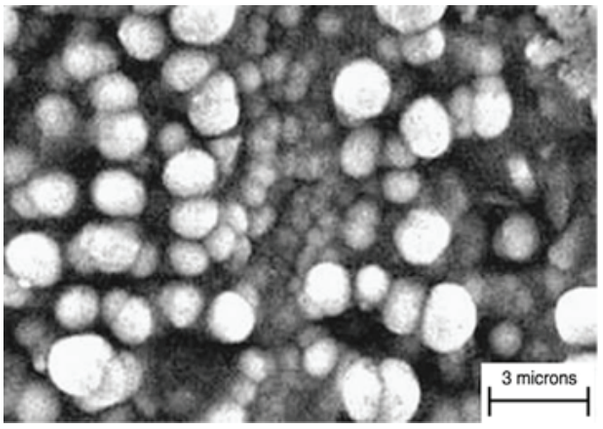


*(a) pure Cr coating*

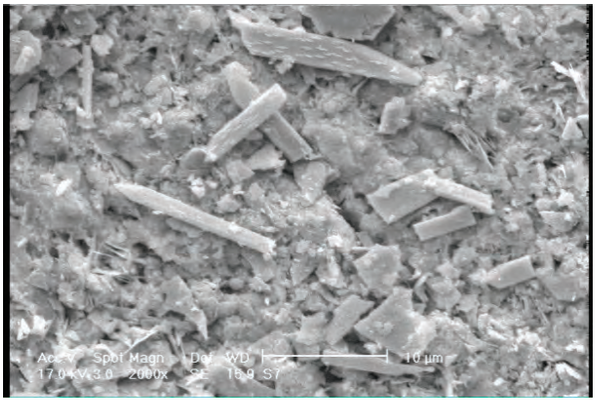


*(b) Cr-nano $TiO_2$ coating*

***Figure 2:*** *SEM surface morphology of (a) Cr and (b) Cr-$TiO_2$ nanocomposite coatings on copper.*

by nail oil and only remained an exposed area for testing. Polarization curves were started after 20 min immersion of samples in the solution.

DC power source was IKA Elektrolyse (ERAM TRONICS, 303D model), using for coating depositing.

### 2.3. Preparation of $TiO_2$ nanoparticles

In a typical preparation by Stucky, G.D. [14], 2 mL of Titanium(IV) chloride (99.9%) was slowly added to anhydrous benzyl alcohol (20 mL) under vigorous stirring at room temperature. The reaction vessel was covered with a Petri dish and under continuous stirring the sol was either kept at 75°C, the aging time was only 24 h. The resulting white suspension was centrifuged. The precipitate was thoroughly washed three times with ethanol (1×20 mL) and THF (2×20 mL). After every washing step, the solvent was removed by centrifugation. The collected material was left to dry in air overnight and then ground into a fine white powder. Calcination of selected samples was performed at 450 °C for 5 h.

### 2.4. Preparation of Cr-$TiO_2$ nanocomposite coating

Pure chromium and Cr–$TiO_2$ coatings were electrolytically deposited from sulphate bath. The bath composition and plating conditions are listed in Table 1.

Analytical grade chemicals and distilled water were used to prepare the plating solution. Prior to plating, the $TiO_2$ nanoparticles of a mean diameter 20 nm were dispersed in the electrolyte. The bath solution was subjected to stirring for 12 h before plating. The electrodeposition process was carried out under galvanostatic condition using a regulated DC power source. The copper specimens were polished mechanically and degreased by acetone in degreased plant followed by water wash and then electropolishing was carried out by sulfuric acid solution.

## 3. RESULTS AND DISCUSSION

### 3.1. Characterization of of $TiO_2$ nanoparticles

The XRD patterns of $TiO_2$ nanoparticles are shown in Figure 1. All diffraction peaks can be assigned to the rutile phase without any indication of other crystalline byproducts. The crystallite size was calculated using Debye–Scherrer equation (Eq.1) [15]:

$$D_c = \frac{K\lambda}{\beta \cos\theta} \qquad (1)$$

where D is the averaged dimension of crystallites, K is the Scherrer constant, somewhat arbitrary value that falls in the range 0.87–1.0 (it is assumed to be 0.9), λ is the incident radiation wavelength, β is the integral breadth of the structurally broadened profile and θ is the angular position. It was shown that the crystal size was 20 nm for $TiO_2$ nanoparticles.

***Table 1:*** *Bath composition and plating conditions for Cr–$TiO_2$ composite coating*

| | |
|---|---|
| $Cr^{3+}$ ion concentration | 1 M |
| Chromium (III) chloride concentration | 260 $g.lit^{-1}$ |
| Anode | Pb ($2\times2\times0.1\ cm^3$) |
| Cathode | Cu ($2\times2\times0.1 cm^3$) |
| pH | 1 (adjusted by $H_2SO_4$) |
| Electroplating time | 15 min |
| current density | 3600 $A/m^2$ |
| Electroplating temperature | 25 °C (R.T.) |
| $TiO_2$ nanoparticles concentration | 5 $g.lit^{-1}$ |

***Table 2:*** *The obtained results on basis Tafel curves of (A) bare (B) Cr coating and (C) Cr- $TiO_2$ nanocomposite on copper in 3.5%NaCl solution*

| **Sample** | **A** | **B** | **C** |
|---|---|---|---|
| $E_{cor}$ (V) | -0.693 | -0.693 | -0.587 |
| $R_p$ (ohm) | 74.9 | 21.14 | 28.37 |
| $i_{cor}$ (A) | $2.902 \times 10^{-4}$ | $1.028 \times 10^{-3}$ | $7.663 \times 10^{-4}$ |
| $I_{cor}$ ($A/cm^2$) | $7.256 \times 10^{-5}$ | $2.571 \times 10^{-4}$ | $1.916 \times 10^{-4}$ |
| Corrosion rate (mpy) | 66.378 | 239.288 | 178.326 |

***Table 3:*** *The obtained results on basis Tafel curves of (A) bare (B) Cr coating and (C) Composite Cr-nano $TiO_2$ on copper in seawater*

| **Sample** | **A** | **B** | **C** |
|---|---|---|---|
| $E_{cor}$ (V) | -0.669 | -0.507 | -0.649 |
| $R_p$ (ohm) | 126.1 | 8.676 | 70.49 |
| $i_{cor}$ (A) | $1.724 \times 10^{-4}$ | $2.605 \times 10^{-3}$ | $3.084 \times 10^{-4}$ |
| $I_{cor}$ ($A/cm^2$) | $4.31 \times 10^{-5}$ | $6.264 \times 10^{-4}$ | $7.71 \times 10^{-5}$ |
| Corrosion rate (mpy) | 39.428 | 583.005 | 71.758 |

***Table 4:*** *The obtained results on basis Tafel curves of (A) bare (B) Cr coating and (C) Composite Cr-nano $TiO_2$ on copper in pipeline water*

| **Sample** | **A** | **B** | **C** |
|---|---|---|---|
| $E_{cor}$ (V) | -0.595 | -0.451 | -0.428 |
| $R_p$ (ohm) | 424.4 | 144.3 | 178 |
| $i_{cor}$ (A) | $5.122 \times 10^{-5}$ | $1.507 \times 10^{-4}$ | $1.221 \times 10^{-4}$ |
| $I_{cor}$ ($A/cm^2$) | $1.281 \times 10^{-5}$ | $3.766 \times 10^{-5}$ | $3.053 \times 10^{-5}$ |
| Corrosion rate (mpy) | 11.718 | 35.051 | 28.415 |

***Table 5:*** *The obtained results on basis Tafel curves of (A) bare (B) Cr coating and (C) Composite Cr-nano $TiO_2$ on copper in distillated water*

| **Sample** | **A** | **B** | **C** |
|---|---|---|---|
| $E_{cor}$ (V) | -0.433 | -0.464 | -0.464 |
| $R_p$ (ohm) | 2671 | 3515 | 2188 |
| $i_{cor}$ (A) | $8.139 \times 10^{-6}$ | $6.185 \times 10^{-6}$ | $9.936 \times 10^{-6}$ |
| $I_{cor}$ ($A/cm^2$) | $2.035 \times 10^{-6}$ | $1.546 \times 10^{-6}$ | $2.484 \times 10^{-6}$ |
| Corrosion rate (mpy) | 1.862 | 1.440 | 2.312 |

### 3.2. Morphological analysis

Figure 2 shows the SEM surface morphology of Cr and composite Cr- $TiO_2$ nanocomposite coatings.
In investigating of Cr and composite Cr-nano $TiO_2$ coating surfaces with scanning electron microscope (SEM), the results showed that the morphology of the coating surface was changed by adding of $TiO_2$ nanoparticles to the chromium coating.
Figure 3 shows the SEM surface morphology of composite Cr- $TiO_2$ nanocomposite coating before and after corrosion.
By corrosion, was carried out a uniform, without crevices, gaps and micron holes film that was prevented from influence corrosive agents on copper surface.

### 3.3. Potentiodynamic polarization measurements

The corrosion behaviors of the mentioned composite coating and the chromium one on the copper surface were compared with the bare copper surface by electrochemical polarization.
Potentiodynamic anodic polarization curves were established. The corrosion rate of the deposits was determined using the Stern–Geary equation (Eq.2) from the polarization measurement [16]:

$$i_{cor} = \frac{\beta_a \beta_c}{2.303 R_p (\beta_a + \beta_c)} \quad (2)$$

Where $i_{corr}$ is the corrosion current density, $R_p$ is the polarization resistance and $\beta_a$ and $\beta_c$ are the anodic and cathodic Tafel slopes. The polarization resistance is calculated on the basis of the following equation (Eq.3):

$$R_p = \frac{\Delta E}{\Delta i} = \frac{dE}{di} \quad (3)$$

The corrosion potential ($E_{corr}$) and corrosion current density ($i_{corr}$) were calculated from the intersection of the cathodic and anodic Tafel curves using the Tafel extrapolation method.
Figure 4 indicates the anodic polarization behavior of bare, pure chromium coated and Cr-nano $TiO_2$ coated copper samples in 3.5% NaCl solution.
The corrosion potential ($E_{cor}$) and corrosion current density ($i_{cor}$) calculated from the intersection of the cathodic and anodic Tafel curves using the Tafel extrapolation method. Based on Tafel curves, the corrosion potential was found to shift from -0.693 V for the bare copper and Cr coating surfaces to more positive amounts of -0.587 V for Cr-nano$TiO_2$ coating. The potential and current of the corrosion, polarization resistance and corrosion rate were calculated and reported in Table. 2
According to the results increasing the corrosion potential to the positive values shows that corrosion begins with delay in the presence of $TiO_2$ nanoparticles. Moreover, adding the $TiO_2$

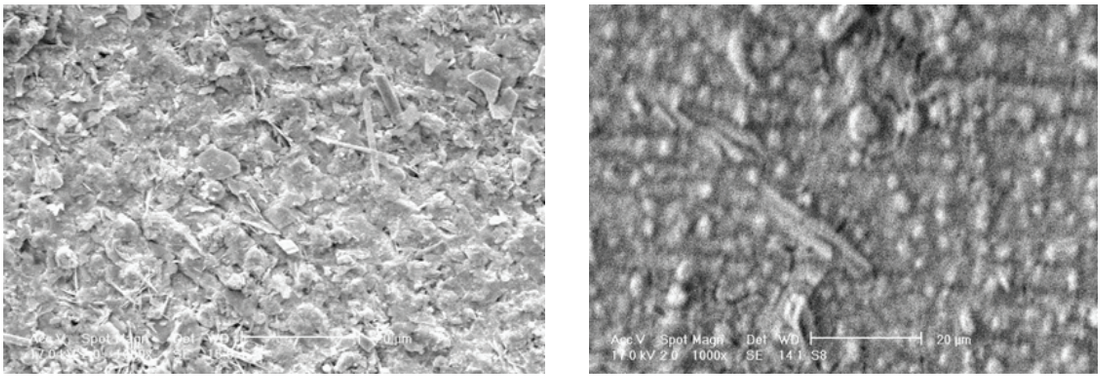


*(a) Before corrosion* *(b) After Corrosion*

***Figure 3:*** *SEM surface morphology of composite Cr-nano $TiO_2$ coating (a) before corrosion (b) after 20 hours immersion in 3.5% NaCl solution on copper.*

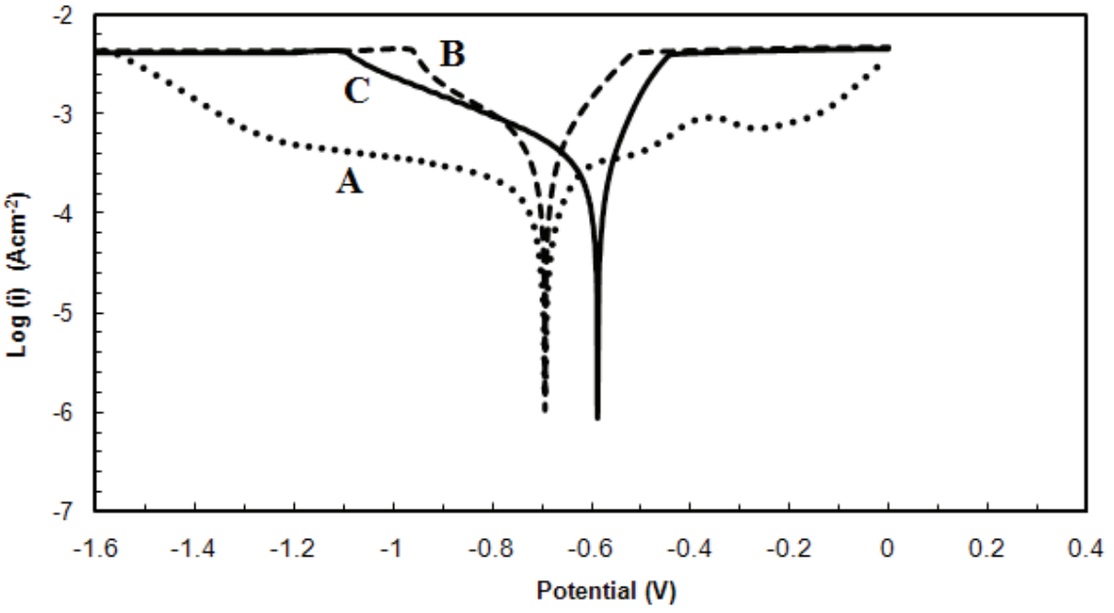


***Figure 4:*** *The Tafel curves of (A) bare (B) Cr coating and (C) composite Cr-nano $TiO_2$ on copper in 3.5%NaCl solution*

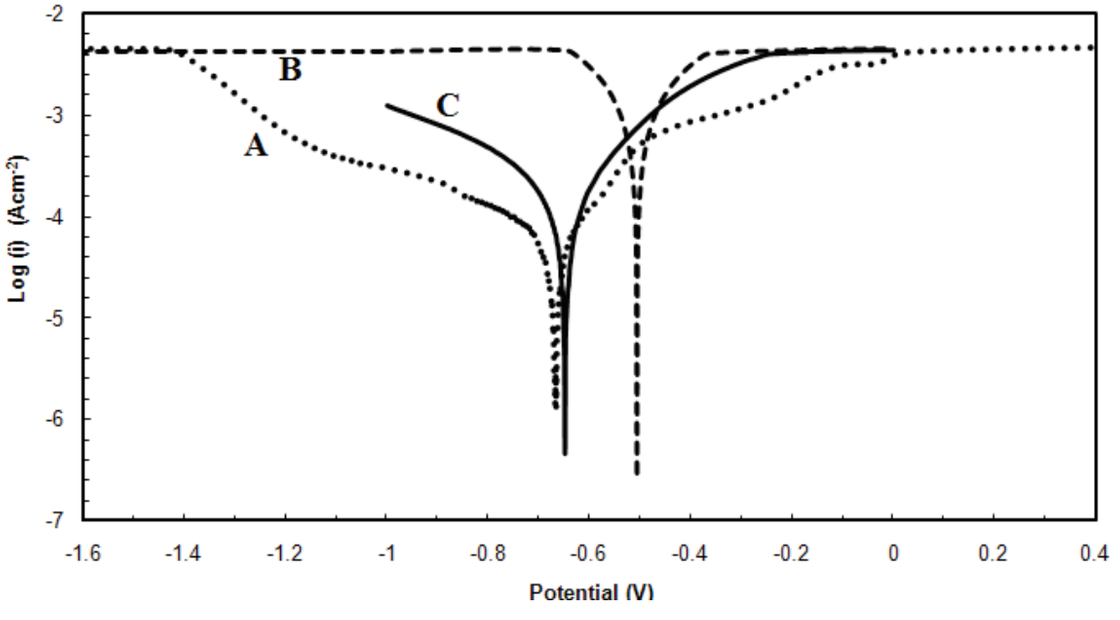


***Figure 5:*** *The Tafel curves of (A) bare (B) Cr coating and (C) composite Cr-nano $TiO_2$ on copper in seawater*

nanoparticles decreased the corrosion current from $2.571\times10^{-4}$ Ampere for chromium coating to $1.916\times10^{-4}$ Ampere for Cr-$TiO_2$ nanocomposite coating. The results showed that adding the $TiO_2$ nanoparticles into chromium coating, caused a decrease in current and rate of corrosion, and so increased the period of conservation from cupric undercoat.

The corrosion resistance of the coatings was investigated by the anodic polarization curves in three other media such as seawater, Zahedan pipeline water and distilled water. Figure 5 shows the anodic polarization behavior of bare, pure chromium coated and Cr-nano $TiO_2$ coated samples in seawater and Table. 3 show the obtained results.

It is known that in chloride media the formation of chloride species is dominant and the dissolution of copper is represented by the two step reaction (Eq.4 and 5), given below.

$$Cu + Cl^- \rightarrow CuCl \quad \text{(slightly soluble)} + e^- \qquad (4)$$

$$CuCl + Cl^- \rightarrow [CuCl_2]^- \quad \text{(soluble complexion)} \qquad (5)$$

On the other hand, the further oxidation of Cu(I) to Cu(II) leads to formation of soluble species like $CuCl_2$ and/or $CuCl^+$ complex ion [17]; Where CuCl is an insoluble adsorbed species,[18-22].

Figure 6 shows the anodic polarization behavior of bare, pure chromium coated and Cr-nano $TiO_2$ coated samples in pipeline water and Table. 4 show the obtained results.

Whereas, cupric and chloride ions were presented in pipeline water; copper tends to corrode readily in the presence of those. The disproportionate reaction is as follows (Eq. 6-9):

$$4Cu+O_2+4H^+ \rightarrow 4Cu^+ + 2H_2O \qquad (6)$$

$$2\,Cu + O_2 + 4H^+ \rightarrow 2Cu^{2+} + 2H_2O \qquad (7)$$

$$Cu^+ + Cl^- \rightarrow CuCl(s) \qquad (8)$$

$$Cu^{2+} + Cu + 2Cl^- \rightarrow 2CuCl(s) \qquad (9)$$

The cuprous chloride complex can further be oxidized to cupric ions, which can again initiate the corrosion of copper by reaction [23].

Figure 7 shows the anodic polarization behavior of bare, pure chromium coated and Cr-nano $TiO_2$ coated samples in distillated water and Table. 5 show the obtained results.

Based on Tafel curves, the uniformly distribution of $TiO_2$ nanoparticles in the chromium coating displaced the potential of the composite coating towards more positive values. Also the corrosion current was found to shift to major values for sample with chromium coatings. It is due to cathodic protective. The corrosion current and rate were decreased with adding $TiO_2$ nanoparticles, thereupon longevity of coatings were increased. According to the results comparison, the minimum and maximum corrosion rates were observed for copper with Cr-$TiO_2$ nanocomposite coating in distillated water and NaCl 3.5% solution, respectively.

## 4. CONCLUSION

Cr–$TiO_2$ nanocomposite coating was generated by electrolytic method. The $TiO_2$ nano-particles were dispersed uniformly in the solution and included in the chromium coating during electrodeposition. The incorporation of $TiO_2$ in the coating led to improvement corrosion resistance of the composite coating as compared to the pure chromium coating. The enhancement in the resistance is due to the physical barriers produced by $TiO_2$ to the corrosion process by filling crevices, gaps and micron holes on the surface of the chromium coating.

The $TiO_2$ uniformly distributed in the chromium coating and displaced the potential of the composite coating towards more positive values. The composite coating exhibits uniform corrosion. This excellent corrosion resistance of the composite coatings provides wide applications in modern industry.

## ACKNOWLEDGEMENT

The authors are thankful to the University of Sistan and Baluchestan (USB) for financial support.

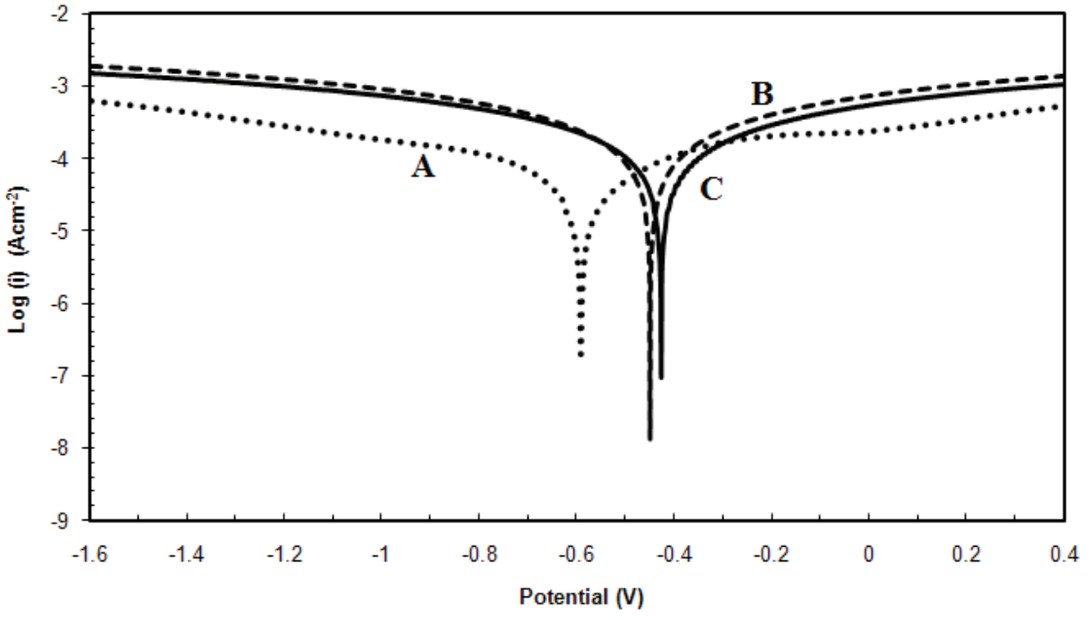


***Figure 6:*** *The Tafel curves of (A) bare (B) Cr coating and (C) composite Cr-nano $TiO_2$ on copper in pipeline water*

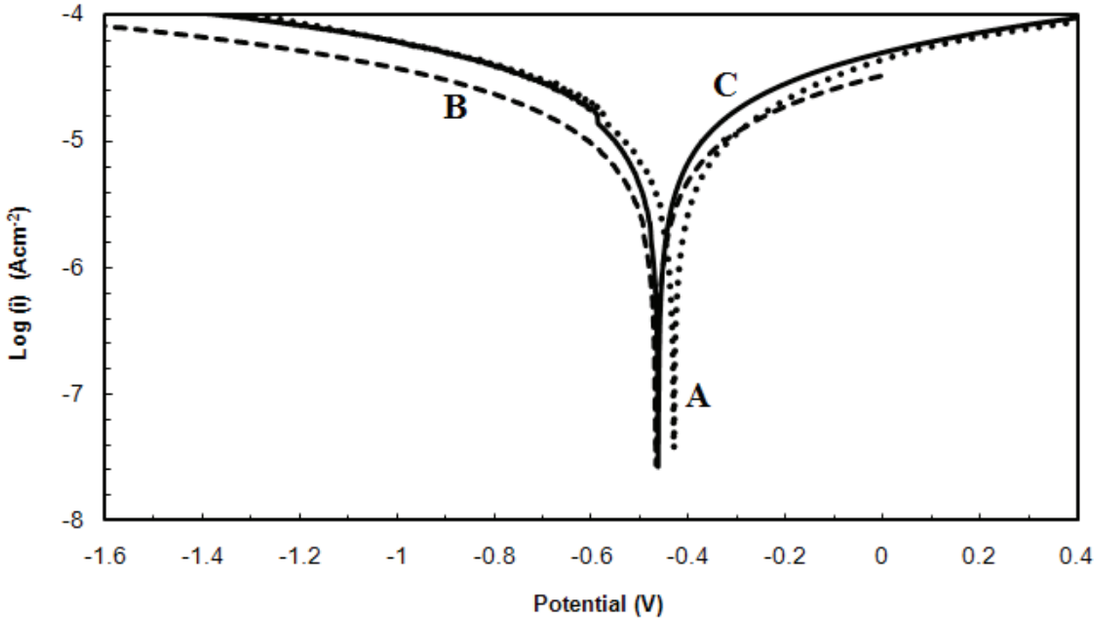


***Figure 7:*** *The Tafel curves of (A) bare (B) Cr coating and (C) composite Cr-nano $TiO_2$ on copper in distillated water*

## REFERENCES


1. A.M. Alfantazi, T.M. Ahmed and D. Tromans: Mater. Design., Vol. 30, No. 7, (2009), pp. 2425-2430.
2. X. Zhang, S.O. Pehkonen, N. Kocherginsky and G.A. Ellis: Corros. Sci., Vol. 44, No. 11, (2002), pp. 2507-2528.
3. E.M. Sherif and S.M. Park: Corros. Sci., Vol. 48, No. 12, (2006), pp. 4065-4079.
4. D.A. Lytle and M.N. Nadagouda: Corros. Sci., Vol. 52, No. 6, (2010), pp. 1927-1938.
5. S. Surviliene, L. Orlovskaja and S. Biallozar: Surf. Coat. Technol., Vol. 122, No. 2-3, (1999), pp. 235-241.
6. G. Saravanan and S. Mohan: Corros. Sci., Vol. 51, No. 1, (2009), pp. 197-202.
7. A.C. Ciubotariu, L. Benea, M. Lakatos-Varsanyi and V .Dragan: Electrochim. Acta., Vol. 53, No. 13, (2008), pp. 4557-4563.
8. Q. Feng, T. li, H. Yue, K. Qi, F. Bai and J. Jin: Appl. Surf. Sci., Vol. 254, No. 8, (2008), pp. 2262-2268.
9. B.M. Praveen and T.V. Venkatesha: Appl. Surf. Sci., Vol. 254, No. 8, (2008), pp. 2418-2424.
10. M.R. Vaezi, S.K. Sadrnezhaad and L. Nikzad: Colloids Surf. A: Physicochem. Eng. Aspects., Vol. 315, No. 1-3, (2008), pp. 176-182.
11. F. Hou, W. Wang and H. Guo: Appl. Surf. Sci., Vol. 252, No. 10, (2006), pp. 3812-3817.
12. R. Subasri, S. Deshpande, S. Seal and T. Shinnohara: Electrochem. Solid State Lett., Vol. 9, No. 1, (2006), pp. B1-B4.
13. K.D. Behler, A. Stravato, V. Mochalin, G. Korneva, G. Yushin and Y. Gogotsi: ACS nano., Vol. 3, No. 2, (2009), pp. 363-369.
14. M. Niederberger, M.H. Bartl and G.D. Stucky: Chem. Mater., Vol. 14, No. 10, (2002), pp. 4364-4370.
15. Q. Feng, T. Li, H. Teng, X. Zhang, Y. Zhang, C. Liu and J. Jin: Surf. Coat. Technol., Vol. 202, No. 17, (2008), pp. 4137-4144.
16. L. Wang, J. Zhang, Z. Zeng, Y. Lin, L. Hu and Q. Xue: Nano. tech., Vol. 17, No. 18, (2006), pp. 4614-4623.
17. T.Tüken: Prog. Org. Coat., Vol. 55, No. 1, (2006), pp. 60-65.
18. H.P. Lee and K. Nobe: J. Electrochem. Soc., Vol. 133, No. 10, (1986), pp. 2035-2043.
19. A. Moreau: Electrochim. Acta., Vol. 26, No. 11, (1981), pp. 1609-1616.
20. A. Moreau, J.P. Frayret, F.D. Rey and R. Pointeau: Electrochim. Acta., Vol. 27, No. 9, (1982), pp. 1281-1291.
21. C. Deslouis, B. Tribollet, G. Mengoli and M.M. Musiani: J. Appl. Electrochem., Vol. 18, No. 3, (1988), pp. 384-393.
22. O.E. Barcia, O.R. Mattos, N. Pebere and B. Tribollet: J. Electrochem. Soc., Vol. 140, No. 10, (1993), pp. 2825-2832.
23. C.M. Chu, C. Lee, Y.Y. Wang, C.C. Wan and C.J. Chen: J. Chin. Inst. Eng., Vol. 38, No. 5-6, (2007), pp. 361-364.